Chameleon Chaotic Systems With Quadratic Nonlinearities: An Adaptive Finite-Time Sliding Mode Control Approach and Circuit Simulation

SALEH MOBAYEN [ID][1,2], **(Member, IEEE), AFEF FEKIH** [ID][3], **(Senior Member, IEEE),**
SUNDARAPANDIAN VAIDYANATHAN [ID][4], **AND ACENG SAMBAS** [ID][5]

[1]Future Technology Research Center, National Yunlin University of Science and Technology, Douliu 64002, Taiwan
[2]Department of Electrical Engineering, Faculty of Engineering, University of Zanjan, Zanjan 45371-38791, Iran
[3]Department of Electrical and Computer Engineering, University of Louisiana at Lafayette, Lafayette, LA 70504, USA
[4]School of Electrical and Computing, Vel Tech University, Chennai 600062, India
[5]Department of Mechanical Engineering, Universitas Muhammadiyah Tasikmalaya, Tasikmalaya 46196, Indonesia

Corresponding author: Saleh Mobayen (mobayens@yuntech.edu.tw)

ABSTRACT A chameleon chaotic system is a chaotic system in which the chaotic attractor can change between hidden and self-excited attractor depending on the values of parameters. In this work, we construct a family of nine new chameleon chaotic systems by introducing two parameters to the 3-D chaotic systems with quadratic nonlinearities and exhibiting line equilibrium points analyzed by Jafari and Sprott (2013). In the analysis of chameleon chaotic flow of the nine new chaotic systems, we discover three categories of hidden attractors (no equilibria, line of equilibria, one stable equilibrium) and a self-excited attractor. The proposed family of nine new chameleon chaotic systems is a novel class of chaotic systems with interesting dynamic properties. Moreover, this study motivates on the adaptive finite time sliding mode control of one category of these chameleon chaotic systems subjected to uncertainties and disturbances. As an engineering application, we have built an electronic circuit design of a new chameleon chaotic system using MultiSim.

INDEX TERMS Chaos, chaotic systems, chameleon systems, adaptive control, circuit design.

I. INTRODUCTION

A chaotic system is a nonlinear dynamical system with three properties, *viz.* (i) sensitive dependence on initial conditions, (ii) topological transitivity, and (iii) dense periodic points [1]. A three-dimensional dissipative autonomous chaotic system is characterized by the existence of positive, zero and negative Lyapunov characteristic exponents with a negative sum of the Lyapunov characteristic exponents [2]. Dynamical systems with chaotic behavior find several applications in areas such as secure communication [3], encryption [4], etc. Attractors in dynamical systems have been recently classified as self-excited attractors and hidden attractors [2]. A self-excited attractor has a basin of attraction that is associated with an unstable equilibrium, while a hidden attractor has a basin of attraction that does not intersect with small neighborhoods of any equilibrium points. Classical chaotic attractors such as Liu system [5], Rucklidge system [6],

Wang system [7] are self-excited attractors. Hidden attractors exist in chaotic systems with no equilibrium points [8]–[10], with only stable equilibrium points [11], [12], with curves of equilibrium points [13]–[15], with surfaces of equilibrium points [16], etc.

A chameleon chaotic system is a chaotic system in which the chaotic attractor can change between hidden and self-excited attractor based on the values of parameters [17]–[20]. Jafari and Sprott [21] found a family of nine chaotic systems with quadratic nonlinearities exhibiting a line of equilibrium points denoted as $LE_1, LE_2, \ldots, LE_9$, respectively. In our research work, we have constructed a family of nine new chameleon chaotic systems by introducing constants a and b to the chaotic systems $LE_1, \ldots, LE_9$ with line equilibrium [21]. We denote the resulting new chameleon chaotic systems as $CH\text{-}LE_1, \ldots, CH\text{-}LE_9$, respectively. We have used Wolf's algorithm [22] to calculate the Lyapunov exponents of the various chaotic systems studied in the work. Whereas the Jafari-Sprott chaotic systems [21] exhibit only a line of equilibrium points, our new family

consists of chameleon chaotic systems displaying a line of equilibrium points, stable equilibrium, unstable equilibrium or no equilibrium based on different values of the parameters. The discovery of nine new chameleon chaotic systems from the Jafari-Sprott systems [21] is a novelty of our research work. Section II describes the new family of nine chameleon chaotic systems.

Control and regulation of chaotic systems are important topics of research in the chaos literature [2]. Various control approaches have been applied in the recent years such as active control [23], [24], fuzzy logic control [25], backstepping control [26], [27], sliding mode control [28]–[30], etc. In Section III, an adaptive finite-time sliding mode control technique is proposed to guarantee the convergence of the state trajectories of the new chameleon chaotic system $CH\text{-}LE_1$ to the origin in the finite time. Numerical simulation results are provided in Section IV to confirm the acceptable performance of the proposed controller on chameleon hidden chaotic systems. Electronic circuit designs of chaotic systems are very useful for engineering applications [31], [32]. In Section V, we have implemented an electronic circuit design of the new chameleon chaotic system $CH\text{-}LE_1$ using MultiSim.

II. CHAMELEON CHAOTIC FLOWS
We start this section with a review of nine chaotic systems with line equilibrium (LE) obtained by Jafari and Sprott [21]. These chaotic systems are denoted as $LE_1, \ldots, LE_9$ [21]. The Jafari-Sprott system LE_1 with line equilibrium [21] is described as follows.

$$\begin{cases} \dot{x}_1 = x_2, \\ \dot{x}_2 = -x_1 + x_2 x_3, \\ \dot{x}_3 = -x_1 - 15x_1 x_2 - x_1 x_3. \end{cases} \tag{1}$$

The Jafari-Sprott system LE_2 with line equilibrium [21] is described as follows.

$$\begin{cases} \dot{x}_1 = x_2, \\ \dot{x}_2 = -x_1 + x_2 x_3, \\ \dot{x}_3 = -x_2 - 17x_1 x_2 - x_1 x_3. \end{cases} \tag{2}$$

The Jafari-Sprott system LE_3 with line equilibrium [21] is described as follows.

$$\begin{cases} \dot{x}_1 = x_2, \\ \dot{x}_2 = -x_1 + x_2 x_3, \\ \dot{x}_3 = x_1^2 - 18x_1 x_2 - x_1 x_3. \end{cases} \tag{3}$$

The Jafari-Sprott system LE_4 with line equilibrium [21] is described as follows.

$$\begin{cases} \dot{x}_1 = x_2, \\ \dot{x}_2 = -x_1 + x_2 x_3, \\ \dot{x}_3 = -4x_1 x_2 - 0.6x_1 x_3 - x_2 x_3. \end{cases} \tag{4}$$

The Jafari-Sprott system LE_5 with line equilibrium [21] is described as follows.

$$\begin{cases} \dot{x}_1 = x_2, \\ \dot{x}_2 = -1.5x_1 + x_2 x_3, \\ \dot{x}_3 = -x_1^2 + x_2^2 - 5x_1 x_2 \end{cases} \tag{5}$$

The Jafari-Sprott system LE_6 with line equilibrium [21] is described as follows.

$$\begin{cases} \dot{x}_1 = x_2, \\ \dot{x}_2 = -x_1 + x_2 x_3, \\ \dot{x}_3 = -0.04x_2^2 - x_1 x_2 - 0.1x_1 x_3. \end{cases} \tag{6}$$

The Jafari-Sprott system LE_7 with line equilibrium [21] is described as follows.

$$\begin{cases} \dot{x}_1 = x_3, \\ \dot{x}_2 = x_1 + x_2 x_3, \\ \dot{x}_3 = 1.85x_1^2 - x_1 x_2 - 0.3x_2 x_3. \end{cases} \tag{7}$$

The Jafari-Sprott system LE_8 with line equilibrium [21] is described as follows.

$$\begin{cases} \dot{x}_1 = x_3, \\ \dot{x}_2 = x_1 - x_2 x_3, \\ \dot{x}_3 = -3x_1^2 + x_1 x_2 + x_1 x_3. \end{cases} \tag{8}$$

The Jafari-Sprott system LE_9 with line equilibrium [21] is described as follows.

$$\begin{cases} \dot{x}_1 = x_3, \\ \dot{x}_2 = -1.62x_2 - x_1 x_3, \\ \dot{x}_3 = x_3 - 0.2x_3^2 + x_1 x_2. \end{cases} \tag{9}$$

In this work, we create a family of nine new 3-D systems by adding constants a and b in the Jafari-Sprott chaotic systems with line equilibrium [21] defined by the equations (1)-(9). We denote the members of the resulting family as $CH\text{-}LE_1, CH\text{-}LE_2, \ldots, CH\text{-}LE_9$, respectively. By dynamic analysis, we show that the new systems are chameleon chaotic systems, *viz.* these systems can change between hidden and self-excited attractors depending on the values of the parameters a and b.

A. THE CHAMELEON CHAOTIC SYSTEM CH-LE₁
By adding constants a and b in the first and second differential equations, respectively, of the Jafari-Sprott system defined by Eq. (1), we obtain the following 3-D system:

$$\begin{cases} \dot{x}_1 = x_2, \\ \dot{x}_2 = -x_1 + x_2 x_3 + a, \\ \dot{x}_3 = -x_1 - 15x_1 x_2 - x_1 x_3 + b, \end{cases} \tag{10}$$

where x_1, x_2, x_3 represent the state variables. Also, a and b denote the constants that determine the dynamic behaviour of the system (10). We choose the initial condition of the system (10) as $(x_1(0), x_2(0), x_3(0)) = (0, 0.5, 0.5)$. We show that the system $CH\text{-}LE_1$ represented by Eq. (10) is a chameleon chaotic system by considering the following four scenarios.

1) LINE OF EQUILIBRIUM POINTS

First, we suppose that $a = 0$ and $b = 0$. Then the system (10) reduces to the system LE_1 [21] defined by Eq. (1). In this special case, the system (10) has a line of equilibrium points, *viz.* all points on the x_3-axis. The Lyapunov exponents of the system (10) were calculated as follows: $\mu_1 = 0.0719$, $\mu_2 = 0$ and $\mu_3 = -0.5232$. This establishes that the system (10) is both chaotic and dissipative in this case.

2) STABLE EQUILIBRIUM

If the condition $a > 0$ and $b = 0$ is satisfied, then the system (10) contains a unique equilibrium point $x_e = [a, 0, -1]^T$. In order to analyze the state trajectories in the vicinity of the equilibrium x_e, the Jacobian matrix of the system (10) at any point $x \in R^3$ is computed as follows:

$$J(x) = \begin{bmatrix} 0 & 1 & 0 \\ -1 & x_3 & x_2 \\ -1 - 15x_2 - x_3 & -15x_1 & -x_1 \end{bmatrix}. \quad (11)$$

For the equilibrium x_e, the Jacobian matrix is determined as follows:

$$J_B = J(x_e) = \begin{bmatrix} 0 & 1 & 0 \\ -1 & -1 & 0 \\ 0 & -15a & -a \end{bmatrix}. \quad (12)$$

The characteristic equation of the matrix J_B is calculated as follows:

$$|\lambda I - J_B| = 0 \Rightarrow (\lambda + a)(\lambda^2 + \lambda + 1) = 0 \quad (13)$$

Solving the characteristic equation (13), we obtain the eigenvalues of J_B as follows:

$$\lambda_1 = -a, \quad \lambda_{2,3} = \frac{-1 \pm j\sqrt{3}}{2} \quad (14)$$

If $a > 0$, then the linearized system for (10) at the equilibrium x_e has a negative real eigenvalue and two complex conjugate eigenvalues with negative real parts. This shows that the equilibrium x_e is a stable focus for the system (10). Figure 1 represents the bifurcation diagram of the system (10). From Figure 1, it is clear that the system (10) has robust chaos for $0 < a < 0.002$ and $b = 0$. When $a = 0.002$ and $b = 0$, the Lyapunov exponents of the system (10) are calculated as $\mu_1 = 0.0908$, $\mu_2 = 0$ and $\mu_3 = -0.5331$. Thus, the system (10) is both chaotic and dissipative. Figure 2 shows the strange chaotic attractor of the system (10) for $a = 0.002$ and $b = 0$.

3) SELF-EXCITED ATTRACTOR

If $a < 0$ and $b = 0$, the system (10) contains a unique equilibrium $x_e = [a, 0, -1]^T$. Similar to Case (2), the eigenvalues of the linearized system (10) at x_e are calculated as follows:

$$\lambda_1 = -a, \quad \lambda_{2,3} = \frac{-1 \pm j\sqrt{3}}{2} \quad (15)$$

Since $a < 0$, $\lambda_1 = -a > 0$. Thus, the equilibrium x_e is an unstable focus. Figure 3 represents the bifurcation diagram
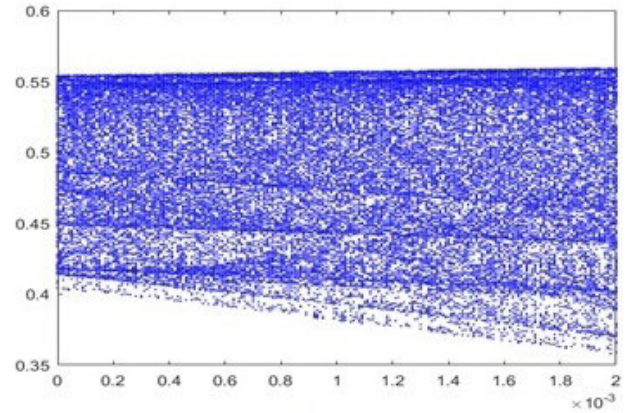

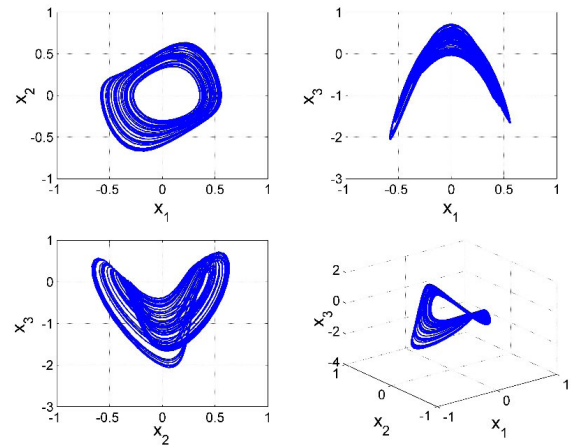**FIGURE 1.** Bifurcation diagram of the system (10) for $0 < a < 0.002$, $b = 0$.

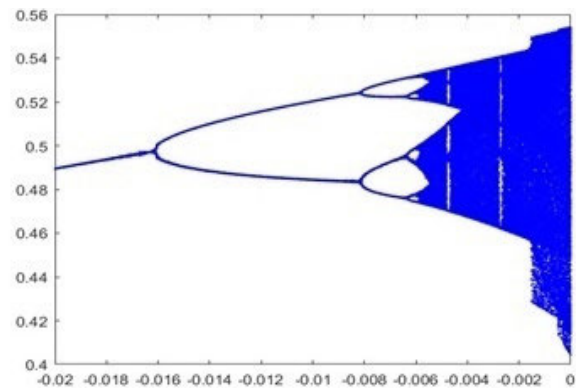**FIGURE 2.** Strange chaotic attractor of the system (10) for $a = 0.002$, $b = 0$.

FIGURE 3. Bifurcation diagram of the system (10) for $-0.02 < a < 0$, $b = 0$.

for the system (10) for $-0.02 < a < 0$ and $b = 0$. From Figure 3, it is clear that the system (10) displays a routine period doubling route to chaos. When $a = -0.002$ and $b = 0$, the Lyapunov exponents of the system (10) were

calculated as $\mu_1 = 0.0654$, $\mu_2 = 0$ and $\mu_3 = -0.5449$. Thus, the system (10) is both chaotic and dissipative.

4) NO EQUILIBRIUM POINT

If $a = 0$ and $b \neq 0$, the system (10) contains no equilibrium point. Figure 4 depicts the bifurcation diagram for the system (10) for $a = 0$ and $-0.02 < b < 0.01$, which demonstrates a routine period doubling route to chaos for the system (10).
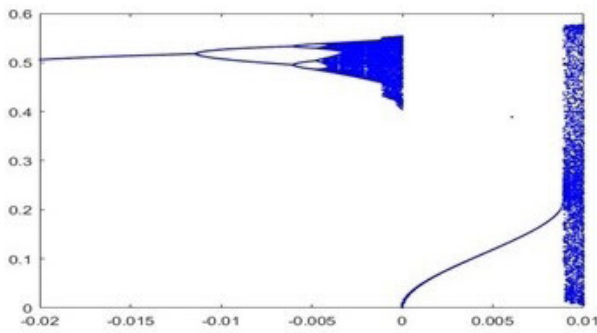

FIGURE 4. Bifurcation diagram of the system (10) for $a = 0$, $-0.02 < b < 0.01$.

When $a = 0$ and $b = 0.01$, the Lyapunov exponents of the system (10) were calculated as $\mu_1 = 0.0480$, $\mu_2 = 0$ and $\mu_3 = -0.2309$. Thus, the system (10) is both chaotic and dissipative. Thus, we have shown that the new system (10) is a chameleon chaotic system, since this system changes between hidden and self-excited attractors depending on the values of a and b.

B. THE CHAMELEON CHAOTIC SYSTEM CH-LE$_2$

By adding constants a and b in the first and second differential equations, respectively, of the Jafari-Sprott system LE_2 defined by Eq. (2), we obtain the following 3-D system:

$$\begin{cases} \dot{x}_1 = x_2, \\ \dot{x}_2 = -x_1 + x_2 x_3 + a, \\ \dot{x}_3 = -x_2 - 17x_1 x_2 - x_1 x_3 + b. \end{cases} \quad (16)$$

where x_1, x_2, x_3 represent the state variables and a, b denote the constants that determine the dynamic behaviour of the system (16). We choose the initial condition of the system (16) as $(x_1(0), x_2(0), x_3(0)) = (0, 0.4, 0)$. We show that $CH\text{-}LE_2$ represented by Eq. (16) is a chameleon chaotic system by considering the following four scenarios.

1) LINE OF EQUILIBRIUM POINTS

First, we suppose that $a = 0$ and $b = 0$. Then the system (16) reduces to the system LE_2 [21] defined by Eq. (2). In this special case, the system (16) has a line of equilibrium points, *viz.* all points on the x_3-axis. The Lyapunov exponents of the system (16) were calculated as follows: $\mu_1 = 0.0574$, $\mu_2 = 0$ and $\mu_3 = -0.2938$. Thus, the system (16) is both chaotic and dissipative.

2) STABLE, MARGINALLY STABLE OR UNSTABLE EQUILIBRIUM

If $a > 0$ and $b = 0$, then the system (16) contains a unique equilibrium point $x_e = [a, 0, 0]^T$. In order to analyze the state trajectories in the vicinity of the equilibrium x_e, the Jacobian matrix of the system (16) at any point $x \in R^3$ is computed as follows:

$$J(x) = \begin{bmatrix} 0 & 1 & 0 \\ -1 & x_3 & x_2 \\ -17x_2 - x_3 & -1 - 17x_1 & -x_1 \end{bmatrix}. \quad (17)$$

For the equilibrium $x_e = [a, 0, 0]^T$, the Jacobian matrix is determined as follows:

$$J_B = J(x_e) = \begin{bmatrix} 0 & 1 & 0 \\ -1 & 0 & 0 \\ 0 & -1 - 17a & -a \end{bmatrix}. \quad (18)$$

The characteristic equation of the matrix J_B is found as

$$|\lambda I - J_B| = 0 \Rightarrow (\lambda + a)(\lambda^2 + 1) = 0. \quad (19)$$

Solving the characteristic equation (19), we obtain

$$\lambda_1 = -a, \quad \lambda = \pm j. \quad (20)$$

Since one eigenvalue is negative and two of eigenvalues are imaginary, the stability of the equilibrium point x_e cannot be determined by Lyapunov's first method. Hence, the equilibrium point x_e of the nonlinear system (16) may be stable, marginally stable or unstable. Figure 5 represents the bifurcation diagram for the system (16) for $0 < a < 0.003$ and $b = 0$. When $a = 0.0006$ and $b = 0$, the Lyapunov exponents of the system (16) were calculated as follows: $\mu_1 = 0.0666$, $\mu_2 = 0$ and $\mu_3 = -0.3022$. Thus, the system (16) is both chaotic and dissipative. Figure 6 shows the strange chaotic attractor of the system (16) for $a = 0.0006$ and $b = 0$.
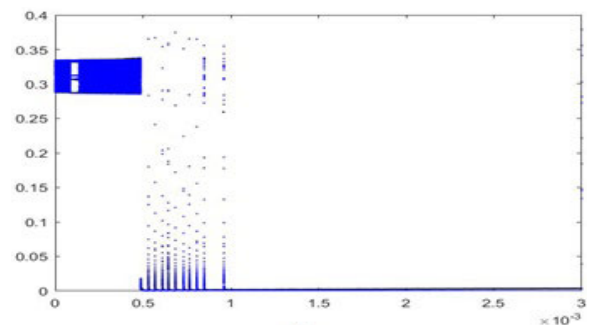

FIGURE 5. Bifurcation diagram of the system (16) for $0 < a < 0.003$, $b = 0$.

3) SELF-EXCITED ATTRACTOR

If $a < 0$ and $b = 0$, the system (16) contains a unique equilibrium point $x_e = [a, 0, 0]^T$. Similar to Case (2), the eigenvalues of the system (16) are easily found as: $\lambda_1 = -a, \lambda_{2,3} = \pm j$. Since $a < 0$, $\lambda_1 = -a > 0$. Thus, the equilibrium
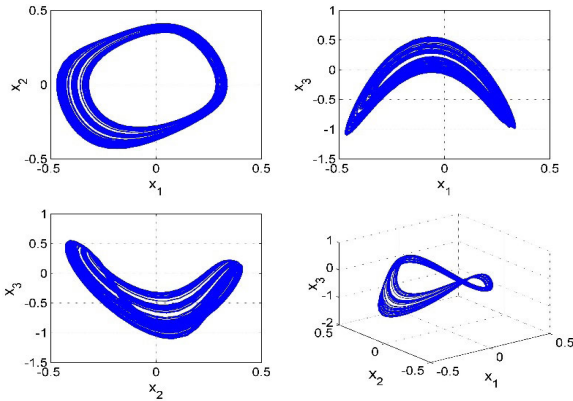
FIGURE 6. Strange chaotic attractor of the system (16) for $a = 0.0006, b = 0.$
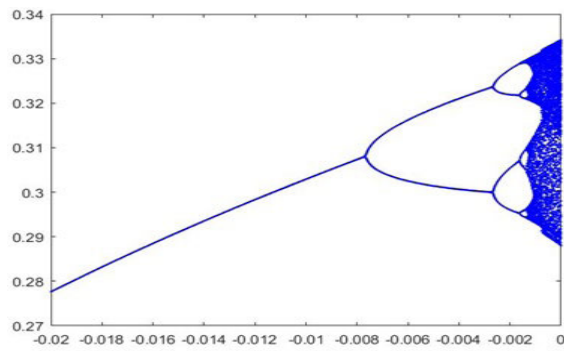

FIGURE 7. Bifurcation diagram of the system (16) for $-0.02 < a < 0, b = 0.$

point x_e is an unstable point. Figure 7 shows the bifurcation diagram for the system (16) for $-0.02 < a < 0$ and $b = 0$. From Figure 7, it is clear that the system (16) displays a routine period doubling route to chaos.

When $a = -0.0006$ and $b = 0$, the Lyapunov exponents of the system (16) were calculated as $\mu_1 = 0.0377$, $\mu_2 = 0$ and $\mu_3 = -0.2772$. Thus, the system (16) is both chaotic and dissipative.

4) NO EQUILIBRIUM POINT
If $a = 0$ and $b \neq 0$, the system (16) contains no equilibrium point. Figure 8 depicts the bifurcation diagram for the system (16) for $a = 0$ and $-0.02 < b < 0$, which demonstrates a routine period doubling route to chaos for the system (16).

When $a = 0$ and $b = -0.0006$, the Lyapunov exponents of the system (16) were calculated as $\mu_1 = 0.0377$, $\mu_2 = 0$ and $\mu_3 = -0.2731$. Thus, the system (16) is both chaotic and dissipative. Thus, we have shown that the system $CH\text{-}LE_2$ (16) is a chameleon chaotic system, since this system changes between hidden and self-excited attractors depending on the values of a and b.

C. THE CHAMELEON CHAOTIC SYSTEM CH-LE₃
By adding constants a and b in the first and second differential equations, respectively, of the Jafari-Sprott system LE_3
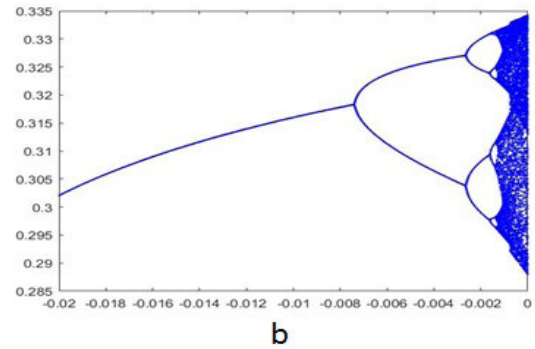

FIGURE 8. Bifurcation diagram of the system (16) for $a = 0, -0.02 < b < 0.$

defined by Eq. (3), we obtain the following 3-D system:

$$\begin{cases} \dot{x}_1 = x_2, \\ \dot{x}_2 = -x_1 + x_2 x_3 + a, \\ \dot{x}_3 = x_1^2 - 18x_1 x_2 - x_1 x_3 + b. \end{cases} \quad (21)$$

where x_1, x_2, x_3 represent the state variables and a, b denote the constants that determine the dynamic behaviour of the system (21). We choose the initial condition of the system (21) as $(x_1(0), x_2(0), x_3(0) = (0, -0.4, 0.5)$. We show that $CH\text{-}LE_3$ represented by Eq. (21) is a chameleon chaotic system by considering the following four scenarios.

1) LINE OF EQUILIBRIUM POINTS
First, we suppose that $a = 0$ and $b = 0$. Then the system (21) reduces to the system LE_3 [21] defined by Eq. (3). In this special case, the system (21) has a line of equilibrium points, viz. all points on the x_3-axis. The Lyapunov exponents of the system (21) were computed as $\mu_1 = 0.0555, \mu_2 = 0$ and $\mu_3 = -0.3243$. Thus, the system (21) is both chaotic and dissipative.

2) SELF-EXCITED ATTRACTOR
If the condition $a > 0$ and $b = 0$ is satisfied, then the system (21) contains a unique equilibrium point $x_e = [a, 0, a]^T$. In order to analyze the state trajectories in the vicinity of the equilibrium x_e, the Jacobian matrix of the system (21) at any point $x \in R^3$ is computed as follows:

$$J(x) = \begin{bmatrix} 0 & 1 & 0 \\ -1 & x_3 & x_2 \\ 2x_1 - 18x_2 - x_3 & -18x_1 & -x_1 \end{bmatrix}. \quad (22)$$

For the equilibrium $x_e = [a, 0, a]^T$, the Jacobian matrix is computed as follows:

$$J_B = J(x_e) = \begin{bmatrix} 0 & 1 & 0 \\ -1 & a & 0 \\ a & -18a & -a \end{bmatrix}. \quad (23)$$

The characteristic equation of the matrix is calculated as follows:

$$|\lambda I - J_B| = 0 \Rightarrow (\lambda + a)(\lambda^2 - a\lambda + 1) = 0. \quad (24)$$

Solving the characteristic equation (24), we obtain the eigenvalues of J_B as follows:

$$\lambda_1 = -a, \quad \lambda_{2,3} = \frac{a \pm \sqrt{a^2 - 4}}{2}. \tag{25}$$

For $0 < a < 2$, we obtain one real negative eigenvalue and two complex eigenvalues with positive real parts. In this case, the equilibrium point x_e is an unstable focus. For $a \geq 2$, we obtain three real eigenvalues with one negative and two positives. In this case, the equilibrium point x_e is an unstable saddle point.

The system (21) is chaotic for $0 < a < 0.0006$ and $b = 0$ as it has a positive Lyapunov exponent for this range of parameters. The Lyapunov exponents of the system (21) were computed as $\mu_1 = 0.0614$, $\mu_2 = 0$ and $\mu_3 = -0.3293$. Thus, the system (21) is both chaotic and dissipative. Figure 9 shows the strange chaotic attractor of the system (21) for $a = 0.0006$ and $b = 0$.
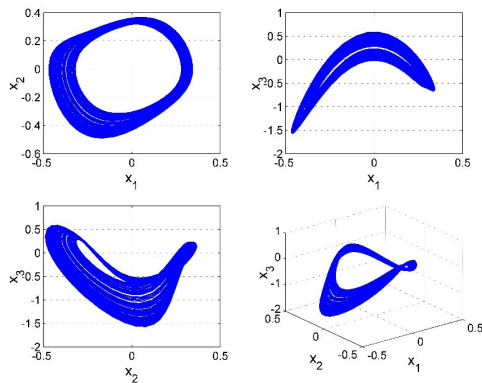

FIGURE 9. Strange chaotic attractor of the system (16) for $a = 0.0006$, $b = 0$.

3) SELF-EXCITED ATTRACTOR
If $a < 0$ and $b = 0$, the system (21) contains a unique equilibrium point $x_e = [a, 0, a]^T$. Similar to Case (2), the eigenvalues of the system (21) are easily found as follows:

$$\lambda_1 = -a, \quad \lambda_{2,3} = \frac{a \pm \sqrt{a^2 - 4}}{2}. \tag{26}$$

Since $a < 0$, $\lambda_1 = -a > 0$. Thus, the equilibrium point x_e is an unstable point. For $-2 < a < 0$, the equilibrium point x_e is a saddle focus, which is unstable. For $a \leq -2$, all the eigenvalues are real with two negative and one positive. In this case, the equilibrium point x_e is an unstable saddle point.

The system (21) is chaotic for $-0.0006 < a < 0$ and $b = 0$ as it has a positive Lyapunov exponent for this range of parameters. When $a = -0.0006$ and $b = 0$, the Lyapunov exponents of the system (21) were computed as $\mu_1 = 0.0377$, $\mu_2 = 0$ and $\mu_3 = -0.3030$. Thus, the system (21) is both chaotic and dissipative.

4) NO EQUILIBRIUM POINT
If $a = 0$ and $b \neq 0$, the system (21) contains no equilibrium point. The system (21) is chaotic for $a = 0$ and $-0.0006 < b < 0$ as it has a positive Lyapunov exponent for this range of parameters. When $a = 0$ and $b = -0.0006$, the Lyapunov exponents of the system (21) were calculated as $\mu_1 = 0.0374$, $\mu_2 = 0$ and $\mu_3 = -0.3032$. Thus, the system (21) is both chaotic and dissipative. Thus, we have shown that the system (21) is a chameleon chaotic system, since this system changes between hidden and self-excited attractors depending on the values of a and b.

D. THE CHAMELEON CHAOTIC SYSTEM CH-LE₄
By adding constants a and b in the first and second differential equations, respectively, of the Jafari-Sprott system LE_4 defined by Eq. (4), we obtain the following 3-D system:

$$\begin{cases} \dot{x}_1 = x_2, \\ \dot{x}_2 = -x_1 + x_2 x_3 + a, \\ \dot{x}_3 = -4x_1 x_2 - 0.6x_1 x_3 - x_2 x_3 + b. \end{cases} \tag{27}$$

where x_1, x_2, x_3 represent the state variables and a, b denote the constants that determine the dynamic behaviour of the system (27). We choose the initial condition of the system (27) as $(x_1(0), x_2(0), x_3(0)) = (0.2, 0.7, 0)$. We show that $CH\text{-}LE_4$ represented by Eq. (27) is a chameleon chaotic system by considering the following four scenarios.

1) LINE OF EQUILIBRIUM POINTS
First, we suppose that $a = 0$ and $b = 0$. Then the system (27) reduces to the system LE_4 [21] defined by Eq. (4). In this special case, the system (27) has a line of equilibrium points, *viz.* all points on the x_3-axis. The Lyapunov exponents of the system (27) were computed as $\mu_1 = 0.0544$, $\mu_2 = 0$, and $\mu_3 = -0.3152$. Thus, the system (27) is both chaotic and dissipative.

2) STABLE, MARGINALLY STABLE OR UNSTABLE EQUILIBRIUM
If the condition $a > 0$ and $b = 0$ is satisfied, then the system (27) contains a unique equilibrium point $x_e = [a, 0, 0]^T$. In order to analyze the state trajectories in the vicinity of the equilibrium x_e, the Jacobian matrix of the system (27) at any point $x \in R^3$ is calculated as follows:

$$J(x) = \begin{bmatrix} 0 & 1 & 0 \\ -1 & x_3 & x_2 \\ -4x_2 - 0.6x_3 & -4x_1 - x_3 & -0.6x_1 - x_2 \end{bmatrix}. \tag{28}$$

For the equilibrium $x_e = [a, 0, 0]^T$, the Jacobian matrix is determined as follows:

$$J_B = J(x_e) = \begin{bmatrix} 0 & 1 & 0 \\ -1 & 0 & 0 \\ 0 & -4a & -0.6a \end{bmatrix}. \tag{29}$$

The characteristic equation of the matrix J_B is calculated as follows:

$$|\lambda I - J_B| = 0 \Rightarrow (\lambda + 0.6a)(\lambda^2 + 1) = 0. \tag{30}$$

Solving the characteristic equation (30), we obtain the eigenvalues of J_B as follows:

$$\lambda_1 = -0.6a, \quad \lambda_{2,3} = \pm j. \tag{31}$$

Since two of the eigenvalues are purely imaginary, the stability of the equilibrium point x_e cannot be determined by Lyapunov's first method. Hence, the equilibrium point x_e may be stable, marginally stable or unstable. The system (27) is chaotic for $0 < a < 0.0006$ and $b = 0$ as it has a positive Lyapunov exponent for this range of parameters.

When $a = 0.0006$ and $b = 0$, the Lyapunov exponents of the system (27) were computed as $\mu_1 = 0.0630$, $\mu_2 = 0$ and $\mu_3 = -0.3227$. Thus, the system (27) is both chaotic and dissipative. Figure 10 shows the strange chaotic attractor of the system (27) for $a = 0.0006$ and $b = 0$.
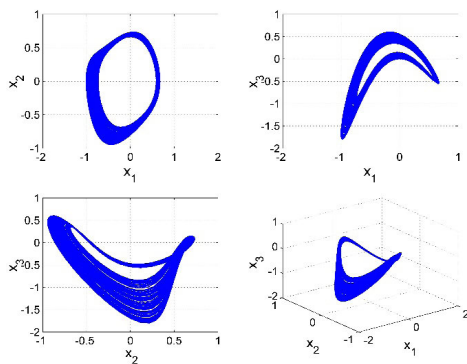

FIGURE 10. Strange chaotic attractor of the system (27) for $a = 0.0006$, $b = 0$.

3) SELF-EXCITED ATTRACTOR

If $a < 0$ and $b = 0$, the system (27) contains a unique equilibrium point $x_e = [a, 0, 0]^T$. Similar to Case (2), the eigenvalues of the system (27) are easily found as follows:

$$\lambda_1 = -0.6a, \quad \lambda_{2,3} = \pm j. \tag{32}$$

Since $a < 0$, $\lambda_1 = -0.6a > 0$. Thus, the equilibrium point x_e is an unstable focus. The system (27) is chaotic for $-0.0006 < a < 0$ and $b = 0$ as it has a positive Lyapunov exponent for this range of parameters. When $a = -0.0006$ and $b = 0$, the Lyapunov exponents of the system (27) were computed as $\mu_1 = 0.0345$, $\mu_2 = 0$ and $\mu_3 = -0.2919$. Thus, the system (27) is both chaotic and dissipative.

4) NO EQUILIBRIUM POINT

If $a = 0$ and $b \neq 0$, then the system (27) contains no equilibrium point. The system (27) is chaotic for $a = 0$ and $-0.0006 < b < 0$ as it has a positive Lyapunov exponent for this range of parameters. When $a = 0$ and $b = -0.0006$, the Lyapunov exponents of the system (27) were calculated as $\mu_1 = 0.0198$, $\mu_2 = 0$ and $\mu_3 = -0.2772$. Thus, the system (27) is both chaotic and dissipative. Thus, we have shown that the system (27) is a chameleon chaotic system, since this system changes between hidden and self-excited attractors depending on the values of a and b.

E. THE CHAMELEON CHAOTIC SYSTEM CH-LE$_5$

By adding constants a and b in the first and second differential equations, respectively, of the Jafari-Sprott system LE_5 defined by Eq. (5), we obtain the following 3-D system:

$$\begin{cases} \dot{x}_1 = x_2, \\ \dot{x}_2 = -1.5x_1 + x_2x_3 + a, \\ \dot{x}_3 = -x_1^2 + x_2^2 - 5x_1x_2 + b. \end{cases} \tag{33}$$

where x_1, x_2, x_3 represent the state variables and a, b denote the constants that determine the dynamic behaviour of the system (33). We choose the initial condition of the system (33) as $(x_1(0), x_2(0), x_3(0)) = (0, 0.1, 0)$. We show that CH-LE_5 represented by Eq. (33) is a chameleon chaotic system by considering the following five scenarios.

1) LINE OF EQUILIBRIUM POINTS

First, we suppose that $a = 0$ and $b = 0$. Then the system (33) reduces to the system LE_5 [21] defined by Eq. (5). In this special case, the system (33) has a line of equilibrium points, *viz.* all points on the x_3-axis. The Lyapunov exponents of the system (33) were computed as $\mu_1 = 0.1390$, $\mu_2 = 0$ and $\mu_3 = -1.3765$. Thus, the system (33) is both chaotic and dissipative.

2) NO EQUILIBRIUM POINT

If $a \neq 0$ and $b = 0$, then the system (33) has no equilibrium point. The system (33) is chaotic for $-0.006 < a < 0.006$ and $b = 0$ as it has a positive Lyapunov exponent for this range of parameters. When $a = 0.006$ and $b = 0$, the Lyapunov exponents of the system (33) were computed as $\mu_1 = 0.0588$, $\mu_2 = 0$ and $\mu_3 = -1.3394$. Thus, the system (33) is both chaotic and dissipative. Figure 11 shows the strange chaotic attractor of the system (33) for $a = 0.006$ and $b = 0$.

FIGURE 11. Strange chaotic attractor of the system (33) for $a = 0.006$, $b = 0$.

3) NO EQUILIBRIUM POINT

If $a = 0$ and $b \neq 0$, then the system (33) has no equilibrium point. The system (33) is chaotic for $a = 0$ and $-0.006 < b < 0.006$, as it has a positive Lyapunov exponent for this

range of parameters. When $a = 0$ and $b = 0.006$, the Lyapunov exponents of the system (33) were calculated as $\mu_1 = 0.1525$, $\mu_2 = 0$ and $\mu_3 = -1.2673$. Thus, the system (33) is both chaotic and dissipative.

4) NO EQUILIBRIUM POINT

If $a \neq 0$ and $b < 0$, then the system (33) has no equilibrium point. The system (33) is chaotic for $-0.006 < a < 0$ or $0 < a < 0.006$ and $-0.006 < b < 0$, as it has a positive Lyapunov exponent for this range of parameters.

5) LINE OF EQUILIBRIUM POINTS

In this case, we suppose that $a \neq 0$ and $b > 0$. If $a^2 \neq 0.75b$, then the system (33) does not have any equilibrium point. In the special case, when $a^2 = 0.75b$, the system (33) contains two lines of equilibrium points, *viz.* $[\sqrt{b}, 0, \alpha]^T$, $(\alpha \in R)$ and $[-\sqrt{b}, 0, \alpha]^T$, $(\alpha \in R)$. It is easy to verify that the system (33) is chaotic for small values of a and b, where $|a| < 0.006$ and $0 < b < 0.006$. Thus, we have shown that the system CH-LE_5 (33) is a chameleon chaotic system, since this system changes between hidden attractors with a line of equilibrium points, two lines of equilibrium points and no equilibrium depending on the values of a and b.

F. THE CHAMELEON CHAOTIC SYSTEM CH-LE₆

By adding constants a and b in the first and second differential equations, respectively, of the Jafari-Sprott system LE_6 defined by Eq. (6), we obtain the following 3-D system:

$$\begin{cases} \dot{x}_1 = x_2, \\ \dot{x}_2 = -x_1 + x_2 x_3 + a, \\ \dot{x}_3 = 0.04 x_2^2 - x_1 x_2 - 0.1 x_1 x_3 + b. \end{cases} \quad (34)$$

where x_1, x_2, x_3 represent the state variables and a, b denote the constants that determine the dynamic behaviour of the system (34). We choose the initial condition of the system (34) as $(x_1(0), x_2(0), x_3(0)) = (1, 2, 0)$. We show that CH-LE_6 represented by Eq. (34) is a chameleon chaotic system by considering the following four scenarios.

1) LINE OF EQUILIBRIUM POINTS

First, we suppose that $a = 0$ and $b = 0$. Then the system (34) reduces to the system LE_6 [21] defined by Eq. (6). In this special case, the system (34) has a line of equilibrium points, *viz.* all points on the x_3-axis. The Lyapunov exponents of the system (34) were computed as $\mu_1 = 0.0543$, $\mu_2 = 0$ and $\mu_3 = -0.6314$. Thus, the system (34) is both chaotic and dissipative.

2) STABLE, MARGINALLY STABLE OR UNSTABLE EQUILIBRIUM

If $a > 0$ and $b = 0$, then the system (34) contains a unique equilibrium point $x_e = [a, 0, 0]^T$. In order to analyze the state trajectories in the vicinity of the equilibrium x_e, the Jacobian matrix of the system (34) at any point $x \in R^3$ is calculated as

follows:

$$J(x) = \begin{bmatrix} 0 & 1 & 0 \\ -1 & x_3 & x_2 \\ -x_2 - 0.1x_3 & 0.08x_2 - x_1 & -0.1x_1 \end{bmatrix}. \quad (35)$$

For the equilibrium $x_e = [a, 0, 0]^T$, the Jacobian matrix is determined as follows:

$$J_B = J(x_e) = \begin{bmatrix} 0 & 1 & 0 \\ -1 & 0 & 0 \\ 0 & -a & -0.1a \end{bmatrix}. \quad (36)$$

The characteristic equation of the matrix J_B is calculated as follows:

$$|\lambda I - J_B| = 0 \Rightarrow (\lambda + 0.1a)(\lambda^2 + 1) = 0. \quad (37)$$

Solving the characteristic equation (37), we obtain the eigenvalues of J_B as follows:

$$\lambda_1 = -0.1a, \quad \lambda = \pm j. \quad (38)$$

Since one eigenvalue is negative and two of eigenvalues are imaginary, the stability of the equilibrium point x_e cannot be determined by Lyapunov's first method. Hence, the equilibrium point x_e of the nonlinear system (16) may be stable, marginally stable or unstable. The system (34) is chaotic for $0 < a < 0.006$ and $b = 0$ as it has a positive Lyapunov exponent for this range of parameters. When $a = 0.006$ and $b = 0$, the Lyapunov exponents of the system (34) were computed as $\mu_1 = 0.0568$, $\mu_2 = 0$ and $\mu_3 = -0.6312$. Thus, the system (34) is both chaotic and dissipative.

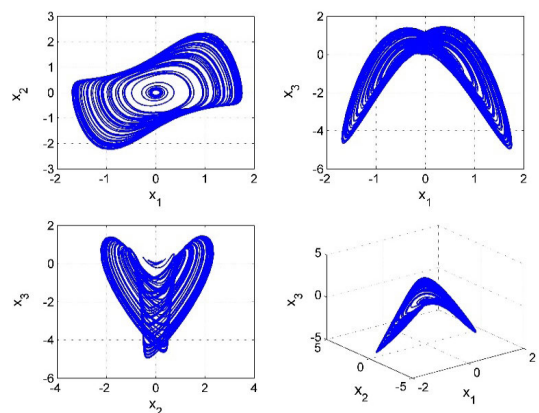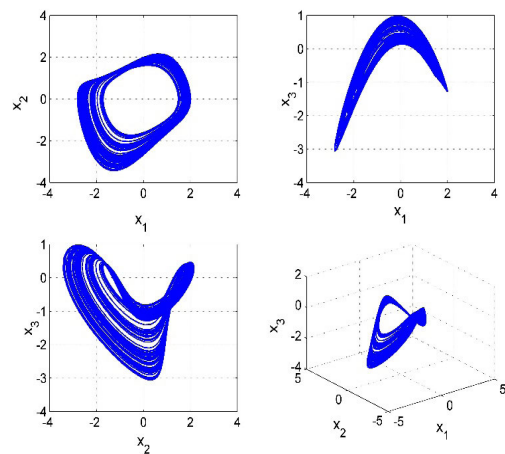Figure 12 shows the strange chaotic attractor of the system (34) for $a = 0.006$ and $b = 0$.

FIGURE 12. Strange chaotic attractor of the system (34) for $a = 0.006$, $b = 0$.

3) SELF-EXCITED ATTRACTOR

If $a < 0$ and $b = 0$, the system (34) contains a unique equilibrium point $x_e = [a, 0, 0]^T$. Similar to Case (2), the eigenvalues of the system (34) are easily found as follows:

$$\lambda_1 = -0.1a, \quad \lambda_{2,3} = \pm j. \quad (39)$$

Since $a < 0$, $\lambda_1 = -0.1a > 0$. Thus, the equilibrium point x_e is an unstable focus. The system (34) is chaotic for $-0.006 < a < 0$ and $b = 0$ as it has a positive Lyapunov exponent for this range of parameters. When $a = -0.006$ and $b = 0$, the Lyapunov exponents of the system (27) were computed as $\mu_1 = 0.0349$, $\mu_2 = 0$ and $\mu_3 = -0.6003$. Thus, the system (34) is both chaotic and dissipative.

4) NO EQUILIBRIUM POINT

If $a = 0$ and $b \neq 0$, the system (34) contains no equilibrium point. The system (34) is chaotic for $a = 0$ and $0 < b < 0.006$, as it has a positive Lyapunov exponent for this range of parameters. When $a = 0$ and $b = 0.006$, the Lyapunov exponents of the system (34) were computed as $\mu_1 = 0.0791$, $\mu_2 = 0$ and $\mu_3 = -0.5009$. Thus, the system (34) is both chaotic and dissipative. Thus, we have shown that the system $CH\text{-}LE_6(34)$ is a chameleon chaotic system, since this system changes between hidden and self-excited attractors depending on the values of a and b.

G. THE CHAMELEON CHAOTIC SYSTEM CH-LE$_7$

By adding constants a and b in the first and second differential equations, respectively, of the Jafari-Sprott system LE_7 defined by Eq. (7), we obtain the following 3-D system:

$$\begin{cases} \dot{x}_1 = x_3, \\ \dot{x}_2 = x_1 + x_2 x_3 + a, \\ \dot{x}_3 = 1.85 x_1^2 - x_1 x_2 - 0.3 x_2 x_3 + b. \end{cases} \quad (40)$$

where x_1, x_2, x_3 represent the state variables and a, b denote the constants that determine the dynamic behaviour of the system (40). We choose the initial condition of the system (40) as $(x_1(0), x_2(0), x_3(0)) = (5.1, 7, 0)$. We show that $CH\text{-}LE_7$ represented by Eq. (40) is a chameleon chaotic system by considering the following four scenarios.

1) LINE OF EQUILIBRIUM POINTS

First, we suppose that $a = 0$ and $b = 0$. Then the system (40) reduces to the system LE_7 [21] defined by Eq. (7). In this special case, the system (40) has a line of equilibrium points, *viz.* all points on the x_2-axis. The Lyapunov exponents of the system (34) were computed as $\mu_1 = 0.0130$, $\mu_2 = 0$ and $\mu_3 = -1.0263$. Thus, the system (40) is both chaotic and dissipative.

2) SELF-EXCITED ATTRACTOR

If $a > 0$ and $b = 0$, then the system (40) contains a unique equilibrium $x_e = [-a, 1.85a, 0]^T$. In order to analyze the state trajectories in the vicinity of the equilibrium x_e, the Jacobian matrix of the system (40) at any point $x \in R^3$ is calculated as follows:

$$J(x) = \begin{bmatrix} 0 & 0 & 1 \\ 1 & x_3 & x_2 \\ 3.7x_1 - x_2 & -x_1 - 0.3x_3 & -0.3x_2 \end{bmatrix}. \quad (41)$$

For the equilibrium x_e, the Jacobian matrix is determined as follows:

$$J_B = J(x_e) = \begin{bmatrix} 0 & 0 & 1 \\ 1 & 0 & 1.85a \\ -5.55a & a & -0.555a \end{bmatrix}. \quad (42)$$

The characteristic equation of the matrix J_B is calculated as follows:

$$\lambda^3 + 0.555a\lambda^2 - 1.85a(a+3)\lambda - a = 0. \quad (43)$$

Since there is a change of sign in the coefficients of the characteristic equation (43), it follows by Routh-Hurwitz criterion that the Jacobian matrix J_B is unstable. Hence, the equilibrium point x_e is unstable. The system (40) is chaotic for $0 < a < 0.0001$ and $b = 0$ as it has a positive Lyapunov exponent for this range of parameters. When $a = 0.0001$ and $b = 0$, the Lyapunov exponents of the system (40) were calculated as follows: $\mu_1 = 0.0197$, $\mu_2 = 0$ and $\mu_3 = -1.0110$. Thus, the system (40) is both chaotic and dissipative. Figure 13 shows the strange chaotic attractor of the system (40) for $a = 0.0001$ and $b = 0$.
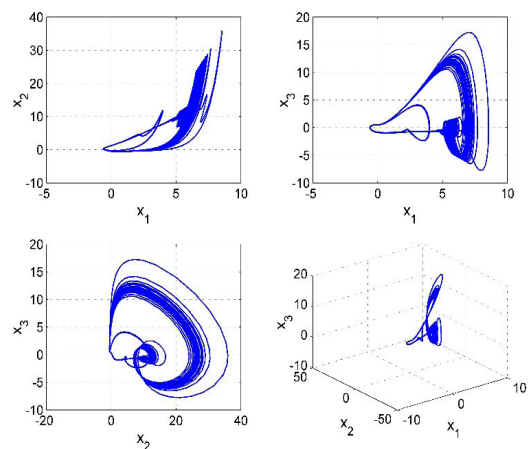

FIGURE 13. Strange chaotic attractor of the system (40) for $a = 0.0001$, $b = 0$.

3) SELF-EXCITED ATTRACTOR

If $a < 0$ and $b = 0$, then the system (40) contains a unique equilibrium $x_e = [-a, 1.85a, 0]^T$. Similar to Case (2), the characteristic equation of the matrix $J_B = J(x_e)$ is calculated as follows:

$$\lambda^3 + 0.555a\lambda^2 - 1.85a(a+3)\lambda - a = 0. \quad (44)$$

Since there is a change of sign in the coefficients of the characteristic equation (44), it follows by Routh-Hurwitz criterion that the Jacobian matrix J_B is unstable. Hence, the equilibrium point x_e is unstable. The system (40) is chaotic for $-0.0001 < a < 0$ and $b = 0$ as it has a positive Lyapunov exponent for this range of parameters. When $a = -0.0001$ and $b = 0$, the Lyapunov exponents of the system (40) were computed as $\mu_1 = 0.0195$, $\mu_2 = 0$ and $\mu_3 = -1.0112$. Thus, the system (40) is both chaotic and dissipative.

4) NO EQUILIBRIUM POINT

If $a = 0$ and $b \neq 0$, the system (40) contains no equilibrium point. The system (40) is chaotic for $a = 0$ and $0 < b < 0.0001$, as it has a positive Lyapunov exponent for this range of parameters. When $a = 0$ and $b = 0.0001$, the Lyapunov exponents of the system (40) were calculated as $\mu_1 = 0.0243$, $\mu_2 = 0$ and $\mu_3 = -1.0147$. Thus, the system (40) is both chaotic and dissipative. Thus, we have shown that the system CH-LE_7 (40) is a chameleon chaotic system, since this system changes between hidden and self-excited attractors depending on the values of a and b.

H. THE CHAMELEON CHAOTIC SYSTEM CH-LE₈

By adding constants a and b in the first and second differential equations, respectively, of the Jafari-Sprott system LE_8 defined by Eq. (8), we obtain the system

$$\begin{cases} \dot{x}_1 = x_3, \\ \dot{x}_2 = x_1 - x_2 x_3 + a, \\ \dot{x}_3 = -3x_1^2 + x_1 x_2 + x_1 x_3 + b. \end{cases} \quad (45)$$

where x_1, x_2, x_3 represent the state variables and a, b denote the constants that determine the dynamic behaviour of the system (45). We choose the initial condition of the system (45) as $(x_1(0), x_2(0), x_3(0)) = (0, -0.3, -1)$. We show that CH-LE_8 represented by Eq. (45) is a chameleon chaotic system by considering the following four scenarios.

1) LINE OF EQUILIBRIUM POINTS

First, we suppose that $a = 0$ and $b = 0$. Then the system (45) reduces to the system LE_8 [21] defined by Eq. (8). In this special case, the system (45) has a line of equilibrium points, *viz.* all points on the x_2-axis. The Lyapunov exponents of the system (45) were computed as $\mu_1 = 0.0535$, $\mu_2 = 0$ and $\mu_3 = -0.8061$. Thus, the system (45) is both chaotic and dissipative.

2) SELF-EXCITED ATTRACTOR

If $a > 0$ and $b = 0$, then the system (45) contains a unique equilibrium $x_e = [-a, 3a, 0]^T$. In order to analyze the state trajectories in the vicinity of the equilibrium x_e, the Jacobian matrix of the system (45) at any point $x \in R^3$ is computed as follows:

$$J(x) = \begin{bmatrix} 0 & 0 & 1 \\ 1 & -x_3 & -x_2 \\ -6x_1 + x_2 + x_3 & x_1 & x_1 \end{bmatrix}. \quad (46)$$

For the equilibrium $x_e = [-a, 3a, 0]^T$, the Jacobian matrix is computed as follows:

$$J_B = J(x_e) = \begin{bmatrix} 0 & 0 & 1 \\ 1 & 0 & -3a \\ 9a & -a & -a \end{bmatrix}. \quad (47)$$

The characteristic equation of the matrix is calculated as follows:

$$\lambda^3 + a\lambda^2 - 3a(a+3)\lambda + a = 0. \quad (48)$$

Since there are two changes of sign in the coefficients of the characteristic equation (48), it follows by Routh-Hurwitz criterion that the equilibrium point x_e is unstable. The system (45) is chaotic for $0 < a < 0.006$ and $b = 0$ as it has a positive Lyapunov exponent for this range of parameters. When $a = 0.006$ and $b = 0$, the Lyapunov exponents of the system (45) were computed as $\mu_1 = 0.0343$, $\mu_2 = 0$ and $\mu_3 = -0.7817$. Thus, the system (45) is both chaotic and dissipative. Figure 14 shows the strange chaotic attractor of the system (45) for $a = 0.006$ and $b = 0$.
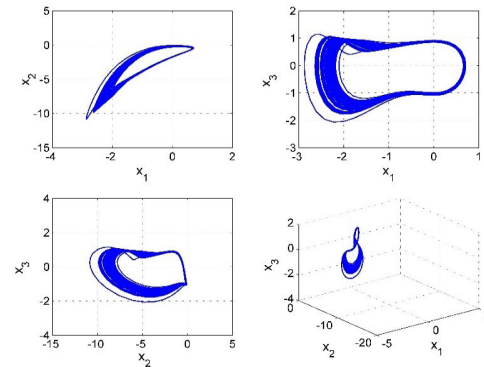

FIGURE 14. Strange chaotic attractor of the system (45) for $a = 0.006, b = 0$.

3) SELF-EXCITED ATTRACTOR

If $a < 0$ and $b = 0$, then the system (45) contains a unique equilibrium $x_e = [-a, 3a, 0]^T$.

Similar to Case (2), the characteristic equation of the matrix $J_B = J(x_e)$ is calculated as follows:

$$|\lambda I - J_B| = 0 \Rightarrow \lambda^3 + a\lambda^2 - 3a(a+3)\lambda + a = 0. \quad (49)$$

Since there are two changes of sign in the coefficients of the characteristic equation (49), it follows by Routh-Hurwitz criterion that the Jacobian matrix J_B is unstable. Hence, the equilibrium point x_e is unstable. The system (45) is chaotic for $-0.006 < a < 0$ and $b = 0$ as it has a positive Lyapunov exponent for this range of parameters. When $a = -0.006$ and $b = 0$, the Lyapunov exponents of the system (45) were computed as $\mu_1 = 0.0474$, $\mu_2 = 0$ and $\mu_3 = -0.8123$. Thus, the system (45) is both chaotic and dissipative.

4) NO EQUILIBRIUM POINT

If $a = 0$ and $b \neq 0$, the system (45) contains no equilibrium point. The system (45) is chaotic for $a = 0$ and $0 < b < 0.006$, as it has a positive Lyapunov exponent for this range of parameters. When $a = 0$ and $b = 0.006$, the Lyapunov exponents of the system (45) were computed as $\mu_1 = 0.0367$, $\mu_2 = 0$ and $\mu_3 = -0.7852$. Thus, the system (45) is both chaotic and dissipative. Thus, we have shown that the system CH-LE_8 (45) is a chameleon chaotic system, since this system changes between hidden and self-excited attractors depending on the values of a and b.

I. THE CHAMELEON CHAOTIC SYSTEM CH-LE$_9$

By adding constants a and b in the first and second differential equations, respectively, of the Jafari-Sprott system LE_9 defined by Eq. (9), we obtain the system

$$\begin{cases} \dot{x}_1 = x_3, \\ \dot{x}_2 = -1.62x_2 - x_1 x_3 + a, \\ \dot{x}_3 = x_3 - 0.2x_3^2 + x_1 x_2 + b. \end{cases} \tag{50}$$

where x_1, x_2, x_3 represent the state variables and a, b denote the constants that determine the dynamic behaviour of the system (50). We choose the initial condition of the system (50) as $(x_1(0), x_2(0), x_3(0)) = (0, 1, 0.8)$. We show that $CH\text{-}LE_9$ represented by Eq. (50) is a chameleon chaotic system by considering the following four scenarios.

1) LINE OF EQUILIBRIUM POINTS

First, we suppose that $a = 0$ and $b = 0$. Then the system (50) reduces to the system LE_9 [21] defined by Eq. (9). In this special case, the system (50) has a line of equilibrium points, *viz.* all points on the x_2-axis. The Lyapunov exponents of the system (50) were computed as $\mu_1 = 0.0642$, $\mu_2 = 0$, and $\mu_3 = -0.6842$. Thus, the system (50) is both chaotic and dissipative.

2) SELF-EXCITED ATTRACTOR

If $a > 0$ and $b = 0$, then the system (50) contains a unique equilibrium $x_e = [0, a/1.62, 0]^T$. In order to analyze the state trajectories in the vicinity of the equilibrium x_e, the Jacobian matrix of the system (50) at any point $x \in R^3$ is computed as follows:

$$J(x) = \begin{bmatrix} 0 & 0 & 1 \\ -x_3 & -1.62 & -x_1 \\ x_2 & x_1 & 1 - 0.4x_3 \end{bmatrix}. \tag{51}$$

For the equilibrium x_e, the Jacobian matrix is determined as follows:

$$J_B = J(x_e) = \begin{bmatrix} 0 & 0 & 1 \\ 0 & -1.62 & 0 \\ a/1.62 & 0 & 1 \end{bmatrix}. \tag{52}$$

The characteristic equation of the matrix is calculated as follows:

$$(\lambda + 1.62)(\lambda^2 - \lambda - a/1.62) = 0. \tag{53}$$

Solving (53), we obtain the eigenvalues

$$\lambda_1 = -1.62, \quad \lambda_{2,3} = \frac{1}{2}\left(1 \pm \sqrt{1 + \frac{4a}{1.62}}\right) \tag{54}$$

Since $a > 0$, the matrix J_B has one positive and two negative eigenvalues. This shows that x_e is an unstable saddle point. The system (50) is chaotic for $0 < a < 0.006$ and $b = 0$ as it has a positive Lyapunov exponent for this range of parameters. When $a = 0.006$ and $b = 0$, the Lyapunov exponents of the system (50) were computed as $\mu_1 = 0.0448$, $\mu_2 = 0$ and $\mu_3 = -0.6662$. Thus, the system (50) is both chaotic and dissipative. Figure 15 shows the
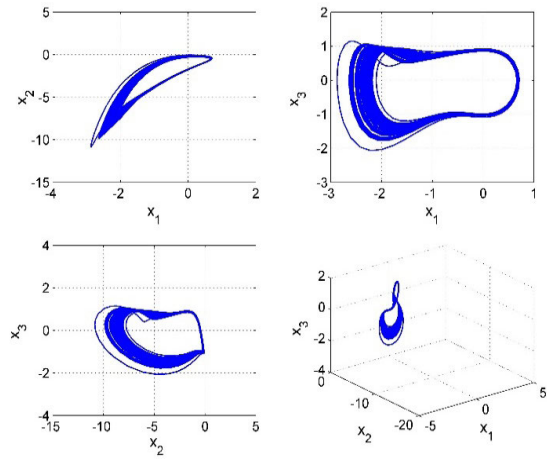
strange chaotic attractor of the system (50) for $a = 0.006$ and $b = 0$.

3) SELF-EXCITED ATTRACTOR

If $a < 0$ and $b = 0$, then the system (50) contains a unique equilibrium $x_e = [0, a/1.62, 0]^T$. Similar to Case (2), the eigenvalues of the linearized system matrix at x_e are easily found as

$$\lambda_1 = -1.62, \quad \lambda_{2,3} = \frac{1}{2}\left(1 \pm \sqrt{1 + \frac{4a}{1.62}}\right) \tag{55}$$

Thus, the equilibrium x_e is an unstable focus for $a < -0.405$ and an unstable saddle point for $a \geq -0.405$. The system (50) is chaotic for $-0.001 < a < 0$ and $b = 0$ as it has a positive Lyapunov exponent for this range of parameters. When $a = -0.001$ and $b = 0$, the Lyapunov exponents of the system (50) were computed as $\mu_1 = 0.0513$, $\mu_2 = 0$ and $\mu_3 = -0.6676$. Thus, the system (50) is both chaotic and dissipative.

4) NO EQUILIBRIUM POINT

If $a = 0$ and $b \neq 0$, the system (50) contains no equilibrium point. The system (50) is chaotic for $a = 0$ and $0 < b < 0.006$, as it has a positive Lyapunov exponent for this range of parameters. When $a = 0$ and $b = 0.006$, the Lyapunov exponents of the system (50) were computed as $\mu_1 = 0.0621$, $\mu_2 = 0$ and $\mu_3 = -0.6836$. Thus, the system (50) is both chaotic and dissipative. Thus, we have shown that the system $CH\text{-}LE_9$ (50) is a chameleon chaotic system, since this system changes between hidden and self-excited attractors depending on the values of a and b.

III. ADAPTIVE FINITE-TIME SLIDING MODE CONTROL

In the present section, the adaptive terminal sliding mode control technique is designed to steer the states of the chameleon chaotic system $CH\text{-}LE_1$ (10) to $\mathbf{0} \in R^3$ in finite time, in spite of uncertain parameter and exterior perturbation.

Remark 1: The proposed controller technique can also be employed on the other new chameleon chaotic systems in a similar manner.

Assuming uncertainties terms in the system dynamics, the chaotic system $CH\text{-}LE_1$ is defined as

$$
\begin{aligned}
\dot{x}_1 &= x_2, \\
\dot{x}_2 &= -x_1 + rx_2x_3, \\
\dot{x}_3 &= -x_1 + qx_1x_2 + sx_1x_3.
\end{aligned} \tag{56}
$$

where q, r and s are the uncertain constants. The chaotic system (56) can be rewritten in matrix notation as

$$
\begin{aligned}
\dot{z}_1 &= A_{11}z_1 + A_{12}z_2 \\
\dot{z}_2 &= A_2z_1 + A_{22}z_2 + Bf(z)\theta + B\eta(z) + Bu
\end{aligned} \tag{57}
$$

where $z_1 \in R^{1\times 1}$ and $z_2 \in R^{2\times 1}$ are the states of the system (57), $\theta \in R^{3\times 1}$ is the uncertainty vector, $\eta(z)$ is the external disturbance, and $u(t)$ is the controller signal. Furthermore, $A_{11}, A_{12}, A_{21}, A_{22}$ and B signify the known matrices and $f(z)$ is the nonlinear function, which are defined as follows:

$$
\begin{aligned}
A_{11} &= 0, \quad A_{12} = \begin{bmatrix} 1 & 0 \end{bmatrix}, \ A_{21} = \begin{bmatrix} -1 \\ -1 \end{bmatrix}, \\
A_{22} &= 0, \quad B = I
\end{aligned} \tag{58}
$$

$$
f(z) = \begin{bmatrix} x_2x_3 & 0 & 0 \\ 0 & x_1x_2 & x_1x_3 \end{bmatrix}, \quad \theta = \begin{bmatrix} r \\ q \\ s \end{bmatrix}. \tag{59}
$$

Assumption 1 [33]: The external disturbance η satisfies the following:

$$
\|\eta(z)\| \le P \|z\| \tag{60}
$$

where $z = (z_1, z_2)$ and P is a positive value.

Assumption 2 [34]: There exist constant matrices with suitable dimensions satisfying:

$$
(A_{11} - A_{12}C_2^{-1}C_1) + (A_{11} - A_{12}C_2^{-1}C_1)^T \le 0 \tag{61}
$$
$$
A_{12}C_2^{-1}C_3 = d \tag{62}
$$

where $C_1 \in R^{2\times 1}, C_2 \in R^{2\times 2}, C_3 \in R^{2\times 1}$ and $d \ge 0$.

Lemma 1 [35]: Consider the positive-definite Lyapunov functional V which fulfills the inequality

$$
V(t) \le -cV(t)^\alpha, \tag{63}
$$

with c as a positive value and α as a fraction of two odd positive integers $(0 < \alpha < 1)$. Hence, for initial time t_0, the Lyapunov functional $V(t)$ converges to origin in finite time

$$
t_s = t_0 + \frac{V^{1-\alpha}(t_0)}{c(1-\alpha)} \tag{64}
$$

where t_s is the settling time.

In the following, we design a fast terminal sliding surface as

$$
\sigma = C_1z_1 + C_2z_2 + C_3\text{sign}(z_1) \tag{65}
$$

where the state trajectories of the chaotic system (57) are on the switching manifold $\sigma = 0$ and converge to the origin in

the finite time. If the system states are reached on the sliding surface, i.e., $\sigma = 0$, we obtain

$$
C_1z_1 + C_2z_2 + C_3\text{sign}(z_1) = 0. \tag{66}
$$

It follows from (66) that

$$
z_2 = -C_2^{-1}\left[C_1z_1 + C_3\text{sign}(z_1)\right] \tag{67}
$$

Substituting (67) into (57), we obtain

$$
\dot{z}_1 = (A_{11} - A_{12}C_2^{-1}C_1)z_1 - A_{12}C_2^{-1}C_3\text{sign}(z_1) \tag{68}
$$

Next, we construct a Lyapunov candidate functional as

$$
V_1(z_1) = z_1^2 \tag{69}
$$

Taking the time-derivative of the above equation and using (68), we have

$$
\dot{V}_1 = 2z_1(A_{11} - A_{12}C_2^{-1}C_1)z_1 - 2z_1A_{12}C_2^{-1}C_3\text{sign}(z_1) \tag{70}
$$

Now, in the light of Assumption 2, we obtain

$$
2z_1(A_{11} - A_{12}C_2^{-1}C_1)z_1 \le 0 \tag{71}
$$

and

$$
2z_1A_{12}C_2^{-1}C_3\text{sign}(z_1) = 2d\,\text{sign}(z_1) = 2d\sqrt{V_1} \tag{72}
$$

Substituting (71) and (72) into (70), we find that

$$
\dot{V}_1 \le -2d\sqrt{V_1} \tag{73}
$$

Then, it can be concluded that z_1 and z_2 converge to the origin in the finite time and based on Lemma 1, the settling time is obtained as

$$
t_s = t_0 + \frac{\sqrt{V_1(t_0)}}{d} \tag{74}
$$

The adaptive terminal sliding mode controller law is proposed to force the state trajectories of (57) to the switching mode surface $\sigma = 0$.

Calculating the time-derivative of (65), we obtain

$$
\dot{\sigma} = C_1\dot{z}_1 + C_2\dot{z}_2 \tag{75}
$$

Using (57) and (68), we get

$$
\begin{aligned}
\dot{\sigma} = C_1 &\left[(A_{11} - A_{12}C_2^{-1}C_1)z_1 - A_{12}C_2^{-1}C_3\text{sign}(z_1)\right] \\
&+ C_2\left[A_2z_1 + A_{22}z_2 + Bf(z)\theta + B\eta(z) + Bu\right] \tag{76}
\end{aligned}
$$

In order to drive on sliding manifold and eliminate the effects of uncertainties and nonlinearities, the controller law is planned as

$$
\begin{aligned}
u = &-(C_2B)^{-1}\left[C_1(R_1z_1 - R_2\text{sign}(z_1))\right] \\
&- B^{-1}(A_{21}z_1 + A_{22}z_2) - f(z)\tilde{\theta} \\
&- (\tilde{P}\|z\| \cdot \|C_2B\| + m)B^{-1}C_2^{-1}\frac{\sigma}{\|\sigma\|} \tag{77}
\end{aligned}
$$

where $R_1 = A_{11} - A_{12}C_2^{-1}C_1, R_2 = A_{12}C_2^{-1}C_3, m$ is a positive value, $\tilde{\theta}$ and $\tilde{P}$ are estimates of θ and P, respectively.

The adaptation laws are given by

$$
\dot{\tilde{\theta}} = \Psi_1 f^T(z)B^T C_2^T \sigma \tag{78}
$$

$$\dot{P} = \Psi_2 \, \|C_2 B\| \, \|z\| \, \|\sigma\| \qquad (79)$$

where $\Psi_1 \in R^{3 \times 3} > 0$ and $\Psi_2 \in R > 0$.

Proof: Construct the Lyapunov candidate function as

$$V_2 = \frac{1}{2}\sigma^T \sigma + \frac{1}{2}(\tilde{\theta} - \theta)^T \Psi_1^{-1}(\tilde{\theta} - \theta)$$
$$+ \frac{1}{2}(\tilde{P} - P)\Psi_2^{-1}(\tilde{P} - P) \qquad (80)$$

Calculating the time-derivative of V_2, we get

$$\dot{V}_2 = \sigma^T \dot{\sigma} + (\tilde{\theta} - \theta)\Psi_1^{-1}\dot{\tilde{\theta}} + (\tilde{P} - P)\Psi_2^{-1}\dot{\tilde{P}} \qquad (81)$$

Substituting (76) into (81), we get the following:

$$\dot{V}_2 = \sigma^T C_1 \left[R_1 z_1 - R_2 \, \text{sign}(z_1) \right]$$
$$+ \sigma^T C_2 \left[A_2 z_1 + A_{22} z_2 + B f(z)\theta + B\eta(z) + Bu \right]$$
$$+ (\tilde{\theta} - \theta)\Psi_1^{-1}\dot{\tilde{\theta}} + (\tilde{P} - P)\Psi_2^{-1}\dot{\tilde{P}} \qquad (82)$$

Substituting (77)-(79) into (82), we get

$$\dot{V}_2 = \sigma^T C_2 B \left\{ f(z)(\theta - \tilde{\theta}) - (\tilde{P} \, \|z\| \cdot \|C_2 B\| + m) B^{-1} C_2^{-1} \frac{\sigma}{\|\sigma\|} \right\}$$
$$+ \sigma^T C_2 B \eta(z) + (\tilde{\theta} - \theta)^T \Psi_1^{-1} \Psi_1 f^T(z) B^T C_2^T \sigma$$
$$+ (\tilde{P} - P)^T \Psi_2^{-1} \Psi_2 \, \|C_2 B\| \, \|z\| \, \|\sigma\|$$

Simplifying, we get

$$\dot{V}_2 = \sigma^T C_2 B \eta(z) - P \, \|C_2 B\| \, \|z\| \, \|\sigma\| - m\sigma^T \frac{\sigma}{\|\sigma\|} \qquad (83)$$

Since $\sigma^T \sigma = \|\sigma\|^2$, we can simplify (83) as follows:

$$\dot{V}_2 = \sigma^T C_2 B \eta(z) - P \, \|C_2 B\| \, \|z\| \, \|\sigma\| - m \, \|\sigma\| \qquad (84)$$

Using Assumption 1, we obtain the following:

$$\dot{V}_2 \leq \|\sigma\| \, \|C_2 B\| \, (\|\eta(z)\| - P \, \|z\|) - m \, \|\sigma\| \leq -m \, \|\sigma\| \qquad (85)$$

Hence, it is concluded from (85) that by the usage of the adaptive input (77) with the parameter estimates (78) and (79), the states of the chaotic system (57) converge to zero in finite time.

IV. SIMULATION RESULTS

In order to confirm the performance of the proposed adaptive finite time sliding mode controller in Section III, numerical simulations are carried out in MATLAB for the chaotic system $CH\text{-}LE_1$.

The system matrices of $CH\text{-}LE_1$ (57) are listed below:

$$A_{11} = 0, \quad A_{12} = \begin{bmatrix} 1 & 0 \end{bmatrix}, \ A_{21} = \begin{bmatrix} -1 \\ -1 \end{bmatrix} \qquad (86)$$

$$A_{22} = \begin{bmatrix} 0 & 0 \\ 0 & 0 \end{bmatrix}, \quad B = \begin{bmatrix} 1 & 0 \\ 0 & 1 \end{bmatrix} \qquad (87)$$

The design parameters of the control input have been selected by trial and error so that the Assumption 2 is satisfied.

We choose the design parameters as follows:

$$m = 2.2, \quad C_1 = \begin{bmatrix} 34 \\ 0 \end{bmatrix}, \ C_2 = \begin{bmatrix} 4 & 0.25 \\ 0.25 & 80 \end{bmatrix} \qquad (88)$$

$$C_3 = \begin{bmatrix} 1 \\ 0.18 \end{bmatrix}, \quad \Psi_1 = \begin{bmatrix} 0.2 & 0.3 & 0.4 \\ 0.3 & 0.5 & 0.4 \\ 0.4 & 0.4 & 0.6 \end{bmatrix} \qquad (89)$$

$$\Psi_2 = 1.5, \quad \eta(z) = \begin{bmatrix} 0.2 z_2 z_3 \sin t \\ 0.2 z_3 \cos t \end{bmatrix}. \qquad (90)$$

In Section III, we defined matrices R_1 and R_2 as

$$R_1 = A_{11} - A_{12} C_2^{-1} C_1, \quad R_2 = A_{12} C_2^{-1} C_3. \qquad (91)$$

A simple calculation in MATLAB shows that
(1) $S = R_1 + R_1^T = -17.0033 < 0$.
(2) $R_2 = A_{12} C_2^{-1} C_3 = 0.2499 > 0$.

Thus, both conditions of Assumption 2 are satisfied for the chosen values of the design parameters. Figure 16 illustrates that the states of $CH\text{-}LE_1$ converge to the origin in the finite time. Figure 17 exhibits the time histories of controller inputs and sliding manifolds. From Figure 17, it is quite clear that the control signals have suitable amplitude and the sliding surfaces converge to origin in finite time even when the disturbances are applied. Moreover, Figure 18 shows the estimation of the uncertain parameters which displays that the final values of estimation parameters are $r = 0.0725$, $q = 0.0952$ and $s = 0.1097$. These simulations prove the success and effectiveness of the proposed adaptive sliding mode control technique.
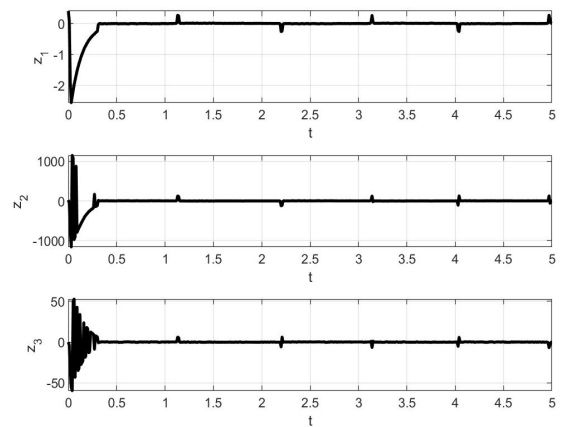

FIGURE 16. Time responses of the controlled states of the system (57).

V. CIRCUIT DESIGN OF THE CHAMELEON CHAOTIC SYSTEM CH-LE$_1$

Using MultiSim, we implement an electronic circuit design of the new chameleon chaotic system $CH\text{-}LE_1$ (Case 2) in this section. The implementation of the chaotic circuit based on the new chameleon chaotic system $CH\text{-}LE_1$ (10) is shown in Figure 19. The circuit consists of three integrators made using the operational amplifiers $U1A$, $U3A$ and $U5A$. For the circuit design, we first scale the variables as follows: $X_1 = 4x_1$, $X_2 = 4x_2$ and $X_3 = 4x_3$. From the new chameleon chaotic system $CH\text{-}LE_1$ (10), we obtain the following
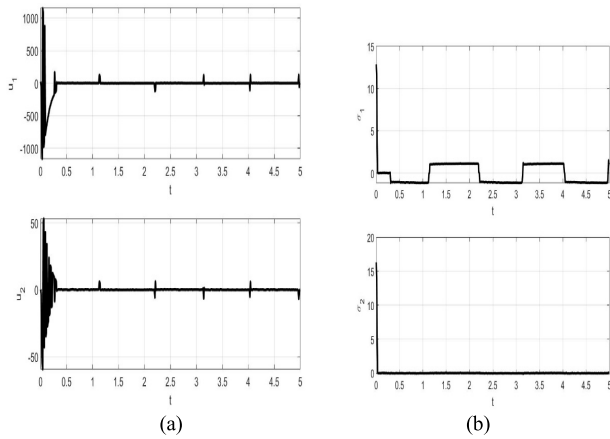
FIGURE 17. Time histories of (a) control signals, and (b) sliding surfaces for the system (57).
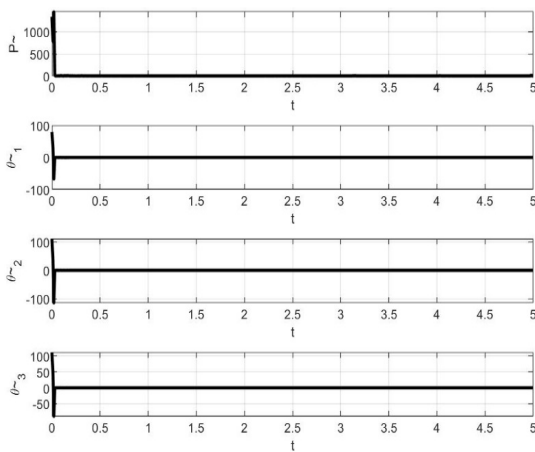

FIGURE 18. Time trajectories of the estimated parameters for the system (57).

dimensionless system:

$$\begin{cases} \dot{X}_1 = X_2 \\ \dot{X}_2 = -X_1 + \dfrac{1}{4}X_2X_3 + a \\ \dot{X}_3 = -X_1 - \dfrac{15}{4}X_1X_2 - \dfrac{1}{4}X_1X_3 \end{cases} \quad (92)$$

By applying Kirchhoff's circuit laws, we get its circuital equations as follows:

$$\begin{cases} \dot{X}_1 = \dfrac{1}{C_1R_1}X_2 \\ \dot{X}_2 = -\dfrac{1}{C_2R_2}X_1 + \dfrac{1}{C_2R_3}X_2X_3 + \dfrac{1}{C_2R_4}V_1 \\ \dot{X}_3 = -\dfrac{1}{C_3R_5}X_1 - \dfrac{1}{C_3R_6}X_1X_2 - \dfrac{1}{C_3R_7}X_1X_3 \end{cases} \quad (93)$$

The values of circuit components have been chosen as follows:

$$\begin{cases} R_1 = R_2 = R_5 = R_8 = R_9 = 10\,k\Omega, \\ R_3 = R_7 = 40\,k\Omega, \quad R_4 = 1250\,k\Omega, \ R_6 = 2.667\,k\Omega, \\ C_1 = C_2 = C_3 = 10\,nF, \quad V_1 = -1\,mV_{DC}. \end{cases} \quad (94)$$
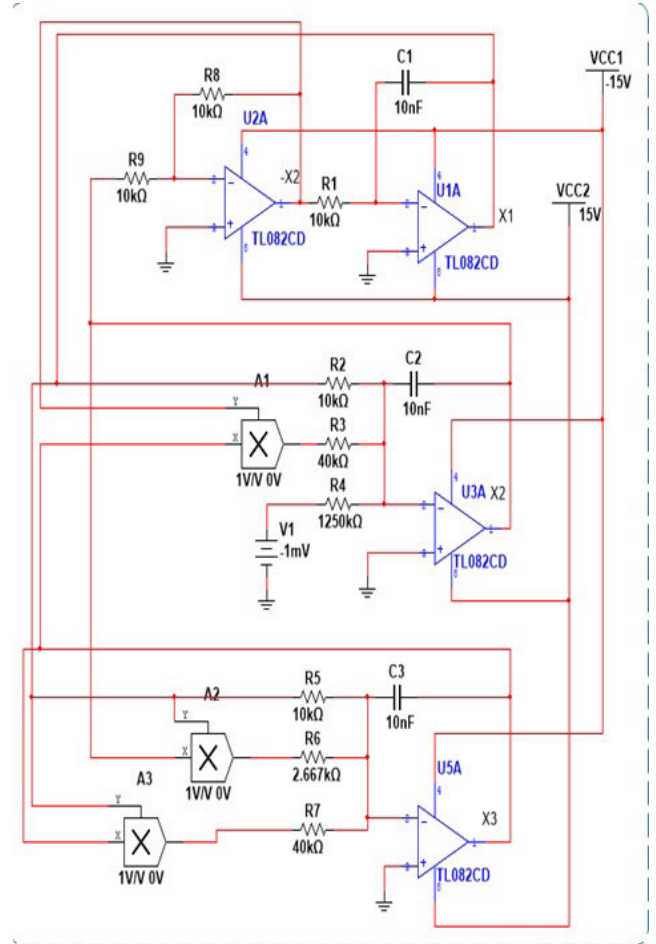
FIGURE 19. The circuit schematic diagram of the new chaotic system CH-LE$_1$ (93).
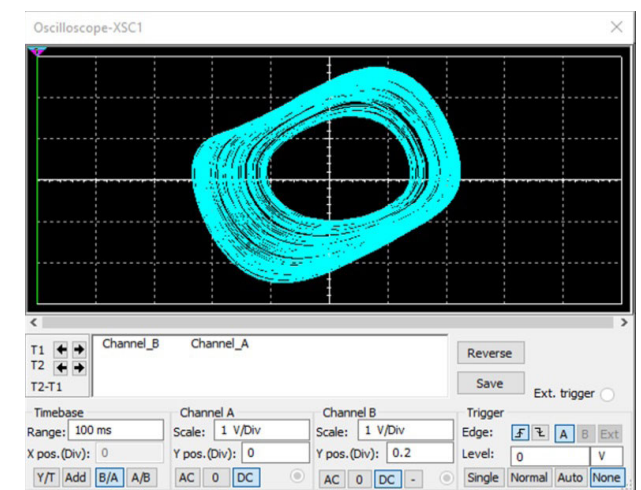

FIGURE 20. The MultiSim output of the system CH-LE$_1$ (93) in the X$_1$-X$_2$ plane.

The MultiSim planar outputs of the circuit (93) are represented in Figures 20-22.

We can observe good similarity between the numerical simulation results as shown in Figure 2 (*CH-LE$_1$*, Case 2) and MultiSim circuit results as shown in Figures 20-22.
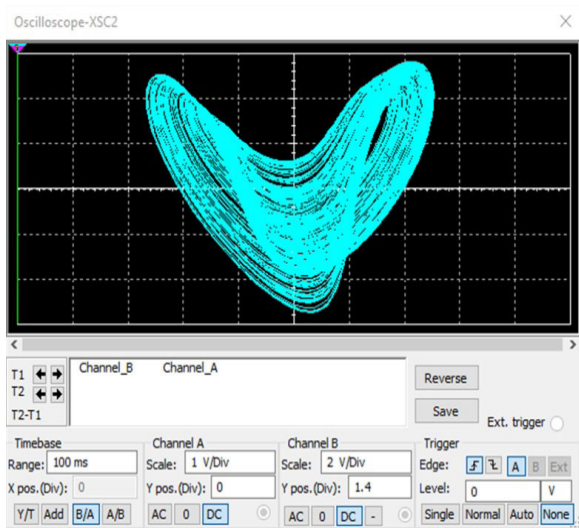
FIGURE 21. The MultiSim output of the system CH-LE$_1$ (93) in the X$_2$-X$_3$ plane.
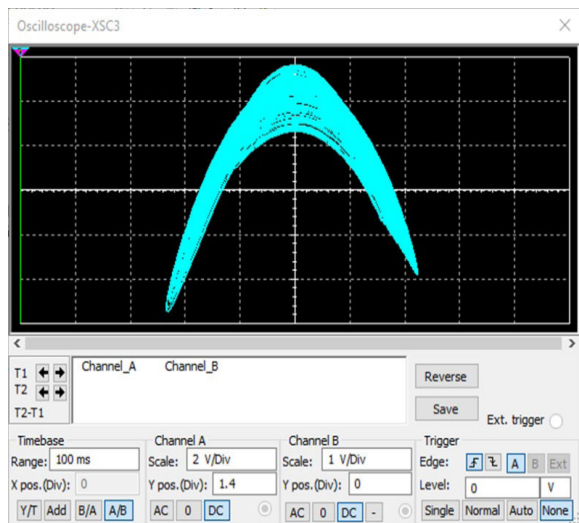

FIGURE 22. The MultiSim output of the system CH-LE$_1$ (93) in the X$_1$-X$_3$ plane.

VI. CONCLUSION

In the chaos literature, chameleon chaotic system is known as a chaotic system in which the chaotic attractor can change between hidden and self-excited attractor depending on the values of parameters. In this work, we constructed a family of nine new chameleon chaotic systems by introducing two parameters to the 3-D chaotic systems with line equilibrium points analyzed by Jafari and Sprott (2013). In the analysis of chameleon chaotic flow of the nine new chaotic systems, we discovered three categories of hidden attractors (no equilibria, line of equilibria, one stable equilibrium) and a self-excited attractor. As a control application, terminal adaptive sliding mode control technique was developed to steer the states of CH-LE$_1$ to the origin in finite time, in spite of uncertainty and exterior perturbations. As an engineering application,

we implemented an electronic circuit design of the new chameleon chaotic system *CH-LE$_1$* using MultiSim.

REFERENCES

[1] R. L. Devaney, *An Introduction to Chaotic Dynamical Systems*. Redwood City, CA, USA: Addison-Wesley, 1989.

[2] V. T. Pham, S. Vaidyanathan, C. Volos and T. Kapitaniak, *Nonlinear Dynamical Systems with Self-Excited and Hidden Attractors*. Berlin, Germany: Springer, 2018.

[3] T. L. Liao, H. C. Chen, C. Y. Peng, and Y. Y. Hou, "Chaos-based secure communications in biomedical information application," *Electronics*, vol. 10, no. 3, pp. 1–19, 2021.

[4] H. Wen, C. Zhang, P. Chen, R. Chen, J. Xu, Y. Liao, Z. Liang, D. Shen, L. Zhou, and J. Ke, "A quantum chaotic image cryptosystem and its application in IoT secure communication," *IEEE Access*, vol. 9, pp. 20481–20492, 2021.

[5] C. Liu, T. Liu, L. Liu, and K. Liu, "A new chaotic attractor," *Chaos, Solitons Fractals*, vol. 22, no. 5, pp. 1031–1038, Dec. 2004.

[6] A. M. Rucklidge, "Chaos in models of double convection," *J. Fluid Mech.*, vol. 237, no. 1, pp. 209–229, Apr. 1992.

[7] J. Wang, Z. Chen, and Z. Yuan, "Existence of a new three-dimensional chaotic attractor," *Chaos, Solitons Fractals*, vol. 42, pp. 3053–3057, 2009.

[8] Z. Wei, "Dynamical behaviors of a chaotic system with no equilibria," *Phys. Lett. A*, vol. 376, no. 2, pp. 102–108, Dec. 2011.

[9] S. Zhang, X. Wang, and Z. Zeng, "A simple no-equilibrium chaotic system with only one signum function for generating multidirectional variable hidden attractors and its hardware implementation," *Chaos, Interdiscipl. J. Nonlinear Sci.*, vol. 30, no. 5, May 2020, Art. no. 053129.

[10] Q. Lai, Z. Wan, and P. D. K. Kuate, "Modelling and circuit realisation of a new no-equilibrium chaotic system with hidden attractor and coexisting attractors," *Electron. Lett.*, vol. 56, no. 20, pp. 1044–1046, Sep. 2020.

[11] M. Molaie, S. Jafari, J. C. Sprott, and S. M. R. H. Golpayegani, "Simple chaotic flows with one stable equilibrium," *Int. J. Bifurcation Chaos*, vol. 23, no. 11, Nov. 2013, Art. no. 1350188.

[12] X. Wang and G. Chen, "A chaotic system with only one stable equilibrium," *Commun. Nonlinear Sci. Numer. Simul.*, vol. 17, no. 3, pp. 1264–1272, Mar. 2012.

[13] S. Mobayen, S. Vaidyanathan, A. Sambas, S. Kaçar, and Ü. Çavuşoğlu, "A novel chaotic system with boomerang-shaped equilibrium, its circuit implementation and application to sound encryption," *Iranian J. Sci. Technol., Trans. Electr. Eng.*, vol. 43, no. 1, pp. 1–12, Mar. 2019.

[14] S. Vaidyanathan, A. Sambas, and M. Mamat, "A new chaotic system with axe-shaped equilibrium, its circuit implementation and adaptive synchronization," *Arch. Control Sci.*, vol. 28, no. 3, pp. 443–462, 2018.

[15] A. Sambas, S. Vaidyanathan, E. Tlelo-Cuautle, S. Zhang, O. Guillen-Fernandez, Y. Hidayat, and G. Gundara, "A novel chaotic system with two circles of equilibrium points: Multistability, electronic circuit and FPGA realization," *Electronics*, vol. 8, no. 11, Oct. 2019, Art. no. 1211.

[16] S. Jafari, J. C. Sprott, and M. Molaie, "A simple chaotic flow with a plane of equilibria," *Int. J. Bifurcation Chaos*, vol. 26, no. 6, Jun. 2016, Art. no. 1650098.

[17] M. A. Jafari, E. Mliki, A. Akgul, V.-T. Pham, S. T. Kingni, X. Wang, and S. Jafari, "Chameleon: The most hidden chaotic flow," *Nonlinear Dyn.*, vol. 88, no. 3, pp. 2303–2317, May 2017.

[18] I. M. Burkin and O. I. Kuznetsova, "On some dynamical chameleon systems," *J. Phys., Conf. Ser.*, vol. 973, Mar. 2018, Art. no. 012052.

[19] K. Rajagopal, A. Akgul, S. Jafari, A. Karthikeyan, and I. Koyuncu, "Chaotic chameleon: Dynamic analyses, circuit implementation, FPGA design and fractional-order form with basic analyses," *Chaos, Solitons Fractals*, vol. 103, pp. 476–487, Oct. 2017.

[20] S. Mobayen, "Design of novel adaptive sliding mode controller for perturbed chameleon hidden chaotic flow," *Nonlinear Dyn.*, vol. 92, no. 4, pp. 1539–1553, Jun. 2018.

[21] S. Jafari and J. C. Sprott, "Simple chaotic flows with a line equilibrium," *Chaos, Solitons Fractals*, vol. 57, pp. 79–84, Dec. 2013.

[22] A. Wolf, J. B. Swift, H. L. Swinney, and J. A. Vastano, "Determining Lyapunov exponents from a time series," *Phys. D, Nonlinear Phenomena*, vol. 16, no. 3, pp. 285–317, Jul. 1985.

[23] F. Xu, P. Yu, and X. Liao, "Global analysis on n-scroll chaotic attractors of modified Chua's circuit," *Int. J. Bifurcation Chaos*, vol. 19, no. 1, pp. 135–157, Jan. 2009.

[24] F. Xu, P. Yu, and X. Liao, "Synchronization and stabilization of multi-scroll integer and fractional order chaotic attractors generated using trigonometric functions," *Int. J. Bifurcation Chaos*, vol. 23, no. 08, Aug. 2013, Art. no. 1350145.

[25] S. Vaidyanathan and A. T. Azar, "Takagi-Sugeno fuzzy logic controller for Liu-Chen four-scroll chaotic system," *Int. J. Intell. Eng. Inform.*, vol. 4, no. 2, pp. 135–150, 2016.

[26] S. Vaidyanathan and A. T. Azar, *Backstepping Control of Nonlinear Dynamical Systems*. Amsterdam, The Netherlands: Elsevier, 2020.

[27] S. Luo, F. L. Lewis, Y. Song, and K. G. Vamvoudakis, "Adaptive back-stepping optimal control of a fractional-order chaotic magnetic-field electromechanical transducer," *Nonlinear Dyn.*, vol. 100, no. 1, pp. 523–540, Mar. 2020.

[28] S. Vaidyanathan and C. H. Lien, *Applications of Sliding Mode Control in Science and Engineering*. Berlin, Germany: Springer, 2017.

[29] G. Piccinni, F. Torelli, and G. Avitabile, "Chaos suppression in forced chaotic systems by innovative sliding mode control," *IEEE Trans. Circuits Syst. II, Exp. Briefs*, vol. 67, no. 8, pp. 1424–1428, Aug. 2020.

[30] Y. N. Golouje and S. M. Abtahi, "Chaotic dynamics of the vertical model in vehicles and chaos control of active suspension system via the fuzzy fast terminal sliding mode control," *J. Mech. Sci. Technol.*, vol. 35, pp. 31–43, Jan. 2021.

[31] A. Sambas, S. Vaidyanathan, E. Tlelo-Cuautle, B. Abd-El-Atty, A. A. A. El-Latif, O. Guillen-Fernandez, Sukono, Y. Hidayat, and G. Gundara, "A 3-D multi-stable system with a peanut-shaped equilibrium curve: Circuit design, FPGA realization, and an application to image encryption," *IEEE Access*, vol. 8, pp. 137116–137132, 2020.

[32] A. Sambas, S. Vaidyanathan, S. Zhang, Y. Zeng, M. A. Mohamed, and M. Mamat, "A new double-wing chaotic system with coexisting attractors and line equilibrium: Bifurcation analysis and electronic circuit simulation," *IEEE Access*, vol. 7, pp. 115454–115462, 2019.

[33] L. Yang and J. Yang, "Robust finite-time convergence of chaotic systems via adaptive terminal sliding mode scheme," *Commun. Nonlinear Sci. Numer. Simul.*, vol. 16, no. 6, pp. 2405–2413, Jun. 2011.

[34] J. Huang, L. Sun, Z. Han, and L. Liu, "Adaptive terminal sliding mode control for nonlinear differential inclusion systems with disturbance," *Nonlinear Dyn.*, vol. 72, nos. 1–2, pp. 221–228, Apr. 2013.

[35] Y. Wang, Y. Feng, X. Yu, and N. Zhang, "Terminal sliding mode control of MIMO linear systems with unmatched uncertainties," in *Proc. 29th Annu. Conf. IEEE Ind. Electron. Soc. (IECON)*, Nov. 2003, pp. 1146–1151.

AFEF FEKIH (Senior Member, IEEE) received the B.S., M.S., and Ph.D. degrees in electrical engineering from the National Engineering School of Tunis, Tunisia, in 1995, 1998, and 2002, respectively. She is currently a Full Professor with the Department of Electrical and Computer Engineering and the Chevron/BORSF Professor of Engineering with the University of Louisiana at Lafayette. Her research interests include control theory and applications, including nonlinear and robust control, optimal control, fault tolerant control with applications to power systems, wind turbines, unmanned vehicles, and automotive engines. She is also a member of the IEEE Control Systems Society and the IEEE Women in Control Society.

SALEH MOBAYEN (Member, IEEE) received the B.Sc. and M.Sc. degrees in control engineering from the University of Tabriz, Tabriz, Iran, in 2007 and 2009, respectively, and the Ph.D. degree in control engineering from Tarbiat Modares University, Tehran, Iran, in January 2013. From February 2013 to December 2018, he was as an Assistant Professor and a Faculty Member with the Department of Electrical Engineering, University of Zanjan, Zanjan, Iran. Since December 2018, he has been an Associate Professor of Control Engineering with the Department of Electrical Engineering, University of Zanjan. He currently collaborates with the National Yunlin University of Science and Technology as an Associate Professor of the Future Technology Research Center. He has published several articles in the national and international journals. His research interests include control theory, sliding mode control, robust tracking, non-holonomic robots, and chaotic systems. He is also a member of the IEEE Control Systems Society and serves as a member of program committee for several international conferences. He is also an Associate Editor of *Artificial Intelligence Review*, *International Journal of Control, Automation and Systems*, *Circuits, Systems, and Signal Processing*, *Simulation*, *Measurement and Control*, *International Journal of Dynamics and Control*, and *SN Applied Sciences*, an Academic Editor of *Complexity* and *Mathematical Problems in Engineering*, and other international journals.

SUNDARAPANDIAN VAIDYANATHAN received the D.Sc. degree in electrical and systems engineering from Washington University in St. Louis, St. Louis, MO, USA, in 1996. He is currently a Professor with the Research and Development Centre, Vel Tech University, Chennai, India. He has published over 480 Scopus-indexed research publications. His current research interests include control systems, chaos theory, mathematical modelling, and scientific computing.

ACENG SAMBAS received the M.Sc. degree in mathematics from Universiti Sultan Zainal Abidin (UniSZA), Malaysia, in 2015. He has been a Lecturer with the Muhammadiyah University of Tasikmalaya, Indonesia, since 2015. His current research interests include dynamical systems, chaotic signals, electrical engineering, computational science, signal processing, robotics, embedded systems, and artificial intelligence.

• • •